NUMERICAL INVESTIGATIONS ON THE RESIDUAL STRESS FIELD IN A CLADDED PLATE DUE TO THE CLADDING PROCESS

Marcus Brand, Jörg Hohe, Dieter Siegele

Fraunhofer-Institute for Mechanics of Materials, Freiburg, Germany

ABSTRACT

The inner surface of reactor pressure vessels is protected against corrosion by an austenitic cladding. Generally, the cladding is welded on the ferritic base metal with two layers to avoid cracks under the cladding and to improve the microstructure of the cladding material. On the other hand, due to the cladding process and the difference of the thermal expansion coefficient of the austenitic cladding and the ferritic base material residual stresses are acting over the wall thickness. This residual stress field is important for the integrity assessment of the component.

For the determination of the residual stress field, plates of a reactor pressure vessel steel were cladded by submerged arc welding and heat treated representative to the real component.. The numerical simulation was performed with the finite element code SYSWELD. The heat source of the model representing the welding process was calibrated against the temperature profiles measured during welding.. In the analysis, the temperature dependent material properties as well as the transformation behavior of the ferritic base metal were taken into account.

The calculated residual stresses show tensile stresses in the cladding followed by compressive stresses in the base metal that are in agreement with measurements with X-ray diffraction technique. After post weld heat treatment the residual stresses in the ferritic base metal are reduced significantly.

Keywords: residual stresses, welding simulation, finite elements.

INTRODUCTION

The integrity of the cladding plays an important role in the safety assessment of reactor pressure vessels (RPV) and reduces the crack driving force of a postulated crack below the cladding. If the cladding is proven to be intact, a crack can be assessed as an internal crack under the cladding (sub-clad cracks) which reduces the stress intensity factor at the crack tip significantly compared to a surface crack [1]. On the other hand, the cladding material shows a much higher toughness than the neighboring base metal and is able to limit the crack extension into RPV wall [2].

For the assessment of postulated sub-clad cracks the residual stress state within the cladding and in the base metal is of importance. These residual stresses result from the bimetallic effect due to the different thermal expansion coefficients of the austenitic cladding and the ferritic base metal and additional stresses from the cladding process itself due to the welding procedure [3]. For the consideration of residual stresses in the cladding different assumptions are present in the literature [4-6]. Summarized measured stress profiles obtained from different measurement techniques often provide different results especially in the region below the cladding. Whereas nondestructive techniques are able to reproduce a

sharp transition between cladding and base metal, destructive methods show a large transition region resulting from the removing of the material [6].

In this investigation, for a submerged arc strip cladding typical for the new generation of German nuclear power plants combined experimental and Finite-Element methods have been applied for the determination of the residual stress profile from the cladding process.

WELDING PROCEDURE

Two plates with the dimension 700 x 300 x 74 mm³ were extracted from a RPV segment of the steel 22 NiMo Cr 37. These plates were cladded with two layers using strip electrodes with the width of 60 mm. The first and the second layer contain 5 strips each.The austenitic cladding material for the first layer has the designation CN 24/13 NBR 800 BS, and for the second layer CrNi 21/10 – BS. The main difference of the materials is a slightly higher content of Chromium in the material of the first layer. The cladding process is a sub-merged arc welding process (SAW) with electrical current of 700 A, a voltage of 28.5 V and a welding speed of 12cm/min. The cladding was performed in PA-position according to DIN EN 287-1. The welding parameters were in accordance with recommendations for the cladding processes in [7] with respect to the filler materials and the interpass temperature. Figure 1 shows one plate after cladding with the indication of the welding direction of the different strips (1st layer: strips 1-5, 2nd layer strips 6-10) and the thermocouples which were spot welded at both sides of the plate for the measurement of the temperature profiles during the cladding process.

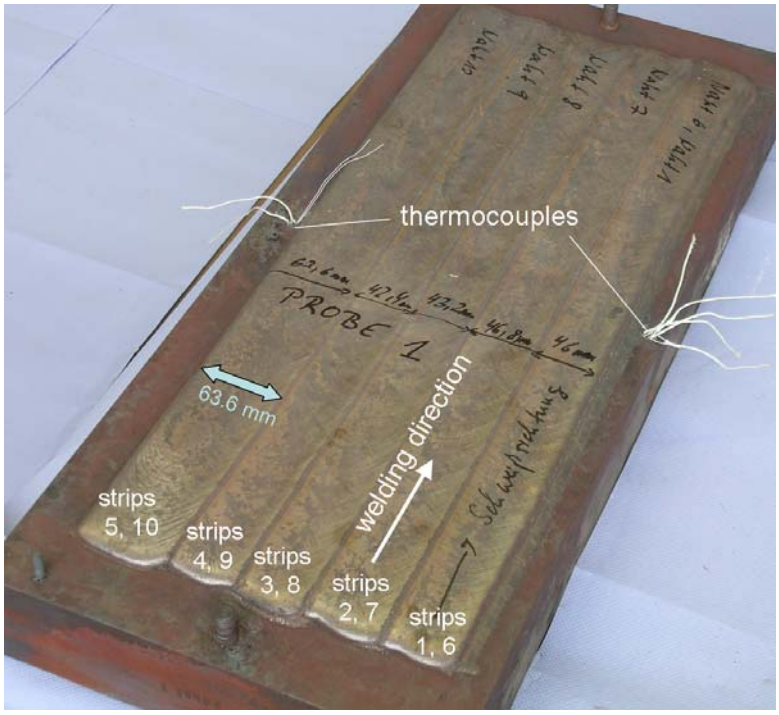

Figure 1: Cladded plate showing the strip welds and the thermocouples used for temperature measurement

The thermocouples were attached in the center of the weld in one line across to the weld and transversal to the direction of the welding sequences. At this position a stationary temperature field can be expected. These temperature measurements are the main basis for the modeling of the heat source within the finite element simulation of the welding process. During welding, the plates were supported in a frame which allows for displacements measurements via clip gages. In addition, the deformation of the plates was measured using the optical object measuring system ARAMIS. The results of the deformation measurements show the expected bending of the plate with the concave side at the cladding which was also found by the numerical simulation.

The cross-section perpendicular through plate after cladding is shown in Figure 2. The two layers of the cladding and the heat affected zone are clearly visible. The maximum thickness of the HAZ is about 10 mm, the thickness of each cladding layer about 4 mm that corresponds to expected values [7]. More details about the boundary conditions of the cladding procedure and the measurement techniques are described in [8].

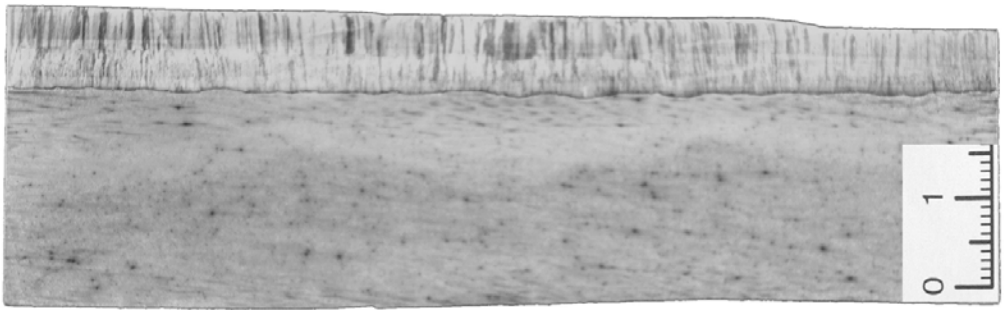

Figure 2: Cross-section through the plate showing the two cladding layers and the HAZ

NUMERICAL WELDING SIMULATION

Numerical methods are nowadays a useful tool for the calculation of distortion and residual stresses as a result from the welding process. Modern finite element codes as SYSWELD [9] which is used for these investigations not only allow for calculation of deformations and stresses due to the welding process but also take into account the change of microstructure due to different heating and cooling rates. In general, the numerical analyses of the transient temperature field and the mechanical analysis are performed in an uncoupled procedure, i.e. the calculated temperature field acts as the load input for the following distortion and stress calculation. This approximation gives reasonable results as long as mechanical deformations do not influence the temperature field in a significant way.

For the welding simulation, the thermo-physical and thermo-mechanical data of the different materials in the range of room temperature to melting temperature have to be known as input data for the analysis. Therefore, physical and mechanical properties of the relevant materials (base metal (BM), heat affected zone (HAZ), and the first and the second layer of the cladding (clad 1, clad 2) have been determined and implemented as a function of temperature in the current FE-analysis (see following chapter). For the simulation of the subsequent heat treatment process the relaxation behavior of the materials has been modeled using a Norton creep law [10].

For the FE-simulation of the transient temperature field all temperature dependent thermo-physical data as the specific heat capacity, the heat conductivity, and the density

were used as input. A three-dimensional moving heat source was applied to the integration points of the 3D FE-model in combination with the birth option to model the material transport from the strip electrode. The heat source itself was approximated for the submerged arc welding process by a cylindrical shape and its axis of rotation corresponding to the width and declination of the strip electrode. As material model an elastic-plastic material with the flow rule according to von Mises was used. The phase transformation which take place in the heat affected zone (HAZ) was considered using the Leblond model [11] for the heating and the Koistinen-Marburger model [12] for the cooling path. The numerical analysis was performed for each strip and cladding layer with the defined welding conditions of the process including the re-melting of the adjoining material zones.

MATERIAL PROPERTIES

The yield stresses and the thermal strains measured by tensile and dilatometer tests throughout the entire temperature range are shown in Figures 3 and 4 for the different materials. From Figure 3 the higher tensile properties of the HAZ compared to the base metal is obvious as well as the lower yield stresses of the cladding materials, whereas the second layer shows significant lower values than the first layer. These differences are partially reduced for the tensile strength.

Figure 4 shows the thermal strain versus temperature for the base metal and the cladding. For the austenitic cladding material a linear relationship exists, whereas for the martensitic base metal a phase transformation is visible which takes place at 728 °C for the heating path and at about 580 °C for the cooling path. The heating and cooling rate in the dilatometer test were 2K/min. Under welding conditions higher heating rates are present which influence the phase transformation temperature. This effect is considered in the numerical welding simulation using the transformation model of Leblond [11].

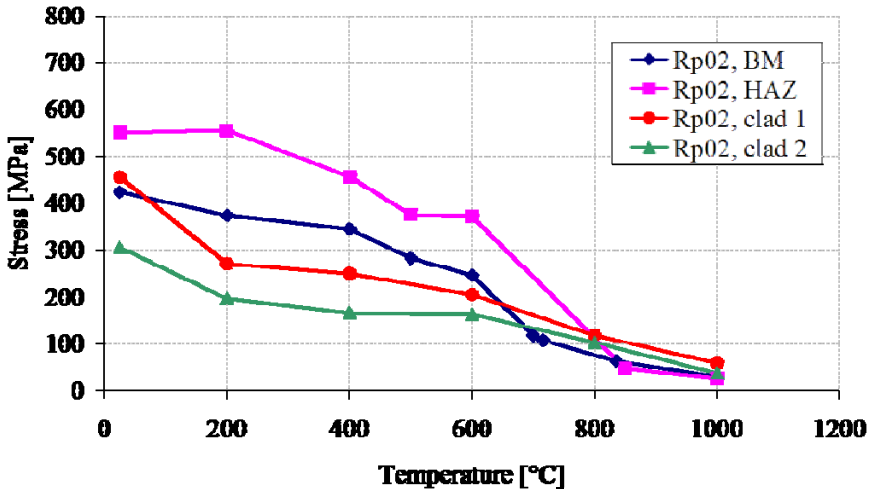

Figure 3: Yield stress $R_{p0.2}$ vs. temperature

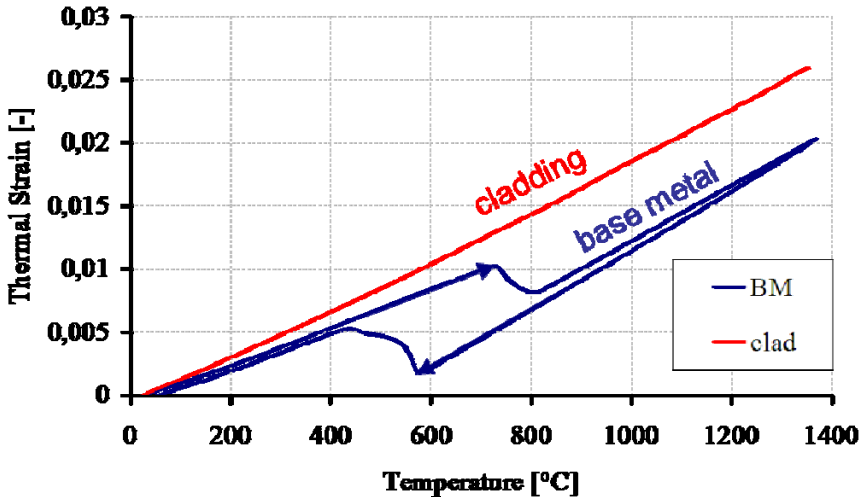

Figure 4: Thermal strain vs. temperature

The creep response of the different material ranges was characterized in relaxation experiments using round tensile specimens of 2.8 mm in diameter. The tests were performed in the temperature range from 450°C to 600°C as the relevant range for the post weld stress–relief heat treatment. In the tests the specimens were loaded with an initial displacement which was kept constant over a time of 20 h and the relaxation of the resulting force was measured. In Figure 5 the results for the base metal (BM) are plotted showing the more pronounced relaxation behavior compared to the cladding material. From the relaxation curves, the parameters for Norton's creep law describing the creep rate as potential function of the applied stress were extracted.

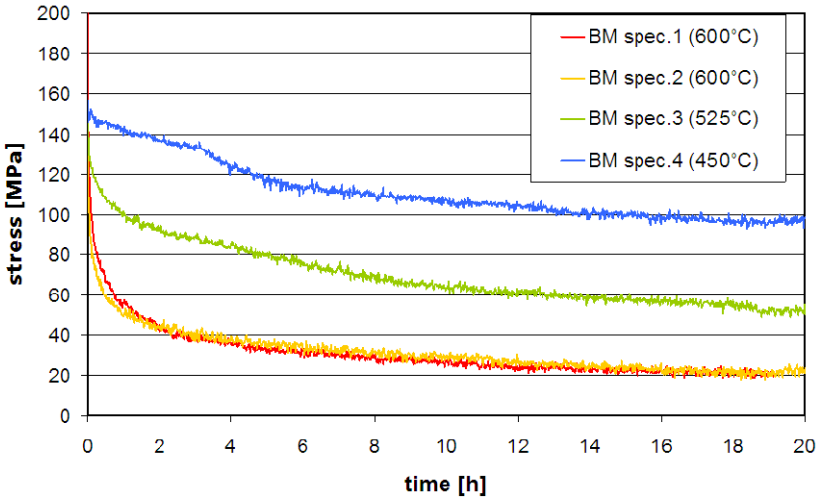

Figure 5: Relaxation behavior of the base metal

CONVERGENCE STUDY

Before the simulation of the full three-dimensional (3D) cladding process, investigations on mesh size and the computation time have been performed on a simplified model with only one strip weld. For symmetry reasons, only one half of the plate has to be modeled. Three different types of meshes (Type I-III) are shown in Figure 6 with increasing mesh density from left to right. The discretisation of the mesh varies in thickness and width direction. For all types of meshes, in the welding zone a maximal element size of 3 mm in length direction was assumed to model a continuous transient temperature field for the given welding speed. For the cladding itself the mesh density is chosen to be constant for all types of meshes.

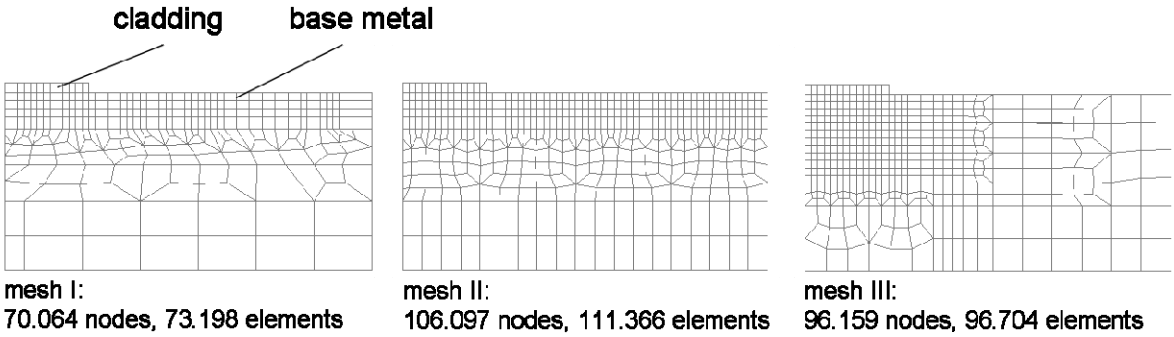

Figure 6: Variation of the mesh density in thickness and width direction

Table 1 shows the maximal deformation at the corner of the model while heating and the maximum shrinkage after cooling. As reference solution, the mesh type III is taken. Whereas a coarse mesh results in negligible difference in the maximal deformation due to heating (1.56%) the difference in shrinkage after cooling down is somewhat higher (-7.57%).

	Type I	Type II	Type III
Maximal deformation in mm	0.195	0.193	0.192
Drift of percentage in %	1.56	0.52	0
Maximum shrinkage in mm	-0.061	-0.063	-0.066
Drift of percentage in %	-7.57	-4.54	0

Table 1 Accuracy of results on transverse deformation

	Type I	Type II	Type III
Maximal deformation in mm	0.719	0.716	0.710
Drift of percentage in %	1.27	0.84	0
Maximum shrinkage in mm	-0.432	-0.434	-0.437
Drift of percentage in %	-1.08	-0.56	0

Table 2 Accuracy of results on longitudinal deformations

The accuracy of the results of the longitudinal deformations at the corner of the model is demonstrated in Table 2. Here, the differences in displacements from the different meshes are much smaller than obtained for the transverse deformations and in summary negligible.

An overview of the remaining longitudinal and transverse residual stresses in the center of the weld after complete cooling is shown in Figures 7 and 8 for the mesh types I-III. Obviously, the mesh with the highest resolution in the cladding region (type III) gives the most accurate result but the residual stresses obtained from the coarser meshes show only small differences. However, 3D FE-simulations of the mechanical behavior (residual stresses) using meshes of type II or III would not run because of the big size of the matrices which are not manageable by 64bit algorithm machines and software using direct solvers at this time. Even an analysis using an iterative solver would lead to unacceptable computation time. Therefore, and because of the small differences in results the mesh Type I was chosen for the full 3D analysis of ten strip welds.

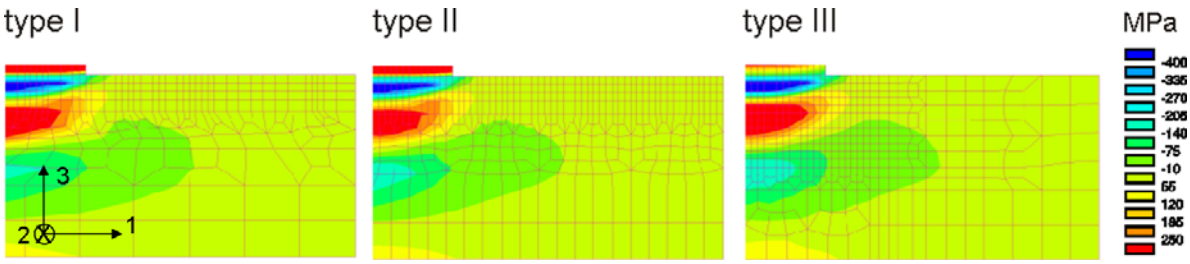

Figure 7: Longitudinal residual stresses σ_{22} after cooling

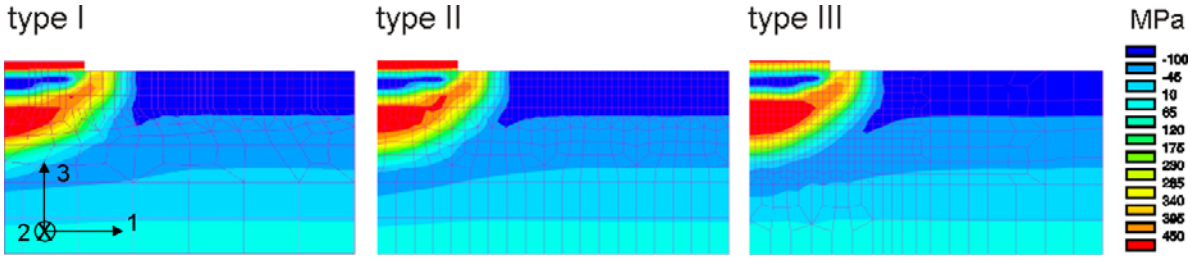

Figure 8: Transverse residual stresses σ_{11} after cooling

SIMULATION OF THE CLADDING PROCESS

Thermal and mechanical analyses of the full cladding process with ten strip welds and two cladding layers were performed with the finite element program SYSWELD. The mesh consists of about 160.400 nodes and 162.300 elements with linear displacement functions. This high resolution is especially necessary for the adequate simulation of the moving heat source.

Figure 9 shows the measured temperature profiles at different positions in comparison with the finite element results for the first strip weld. The highest temperature is obtained at a position being closest to the weld and the peak temperatures decrease with decreasing distance from the weld. As demonstrated in Figure 9, the cooling rates are in very good agreement, whereas the peak temperatures show some small differences which are mainly caused by the fluctuating fusion line due to weld bead forming of the first weld. An excellent agreement of calculation vs. measurement could be achieved on the third strip weld, Fig. 10.

Based on this agreement a simulation result close to the real welding process is expected as demonstrated in former investigations [13].

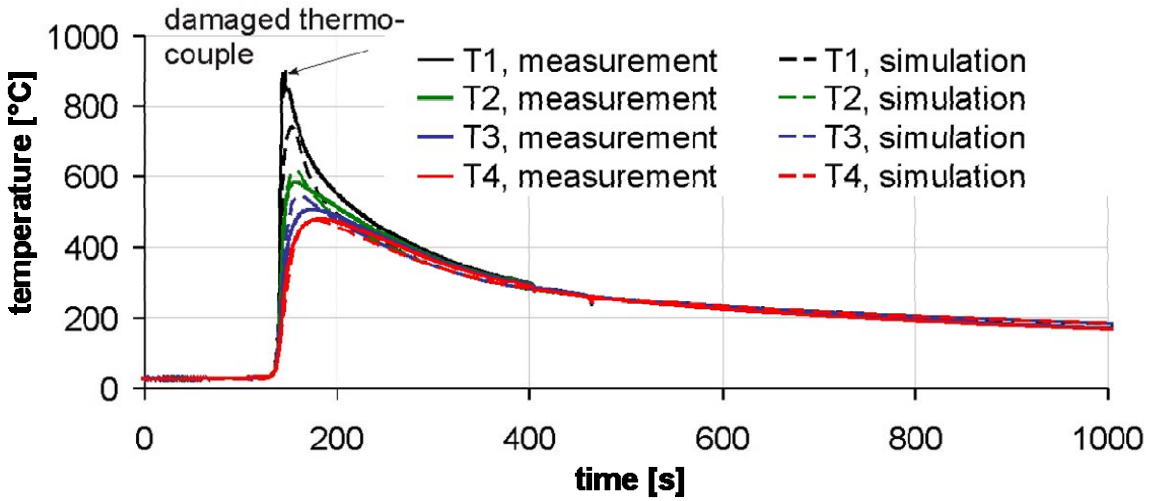

Figure 9: Calculated temperature profiles in comparison with the measurements (1st strip)

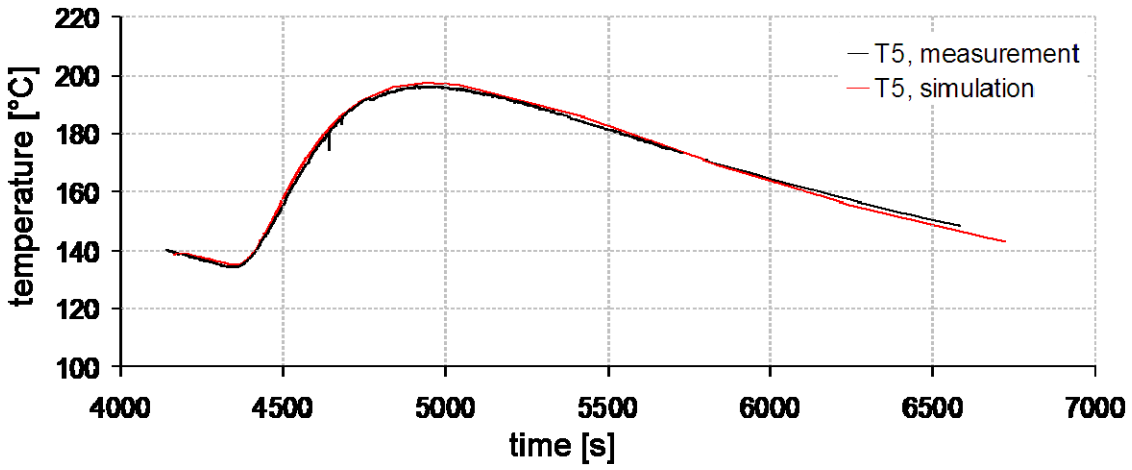

Figure 10: Temperature over time against measurements of the 3rd strip on thermocouple T5.

The calculated longitudinal residual stresses σ_{22} after the welding of ten strip welds and two layers are plotted in Figures 11. The longitudinal stresses show tensile stresses in the cladding and compressive stresses below the cladding followed by tensile stresses in the wall of the plate. It can be seen that each following weld strip weld influences the preceding one in a positive way by a further reduction of the stress level. The transverse stresses across the weld direction show the same behavior with some smaller stress levels, see plots on the left in Figure 12.

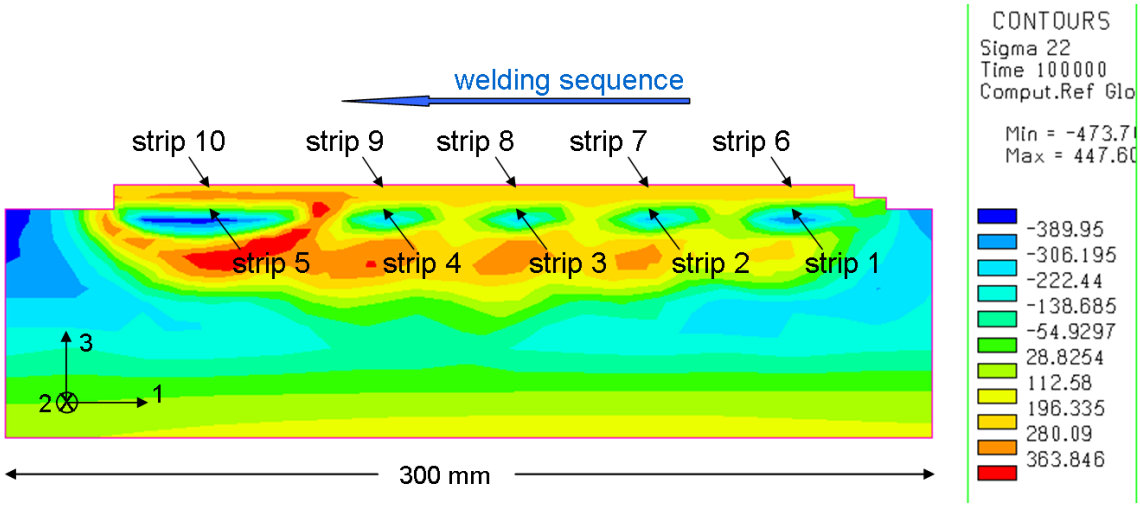

Figure 11: Longitudinal residual stresses in the center of the plate (welding sequence from right to left)

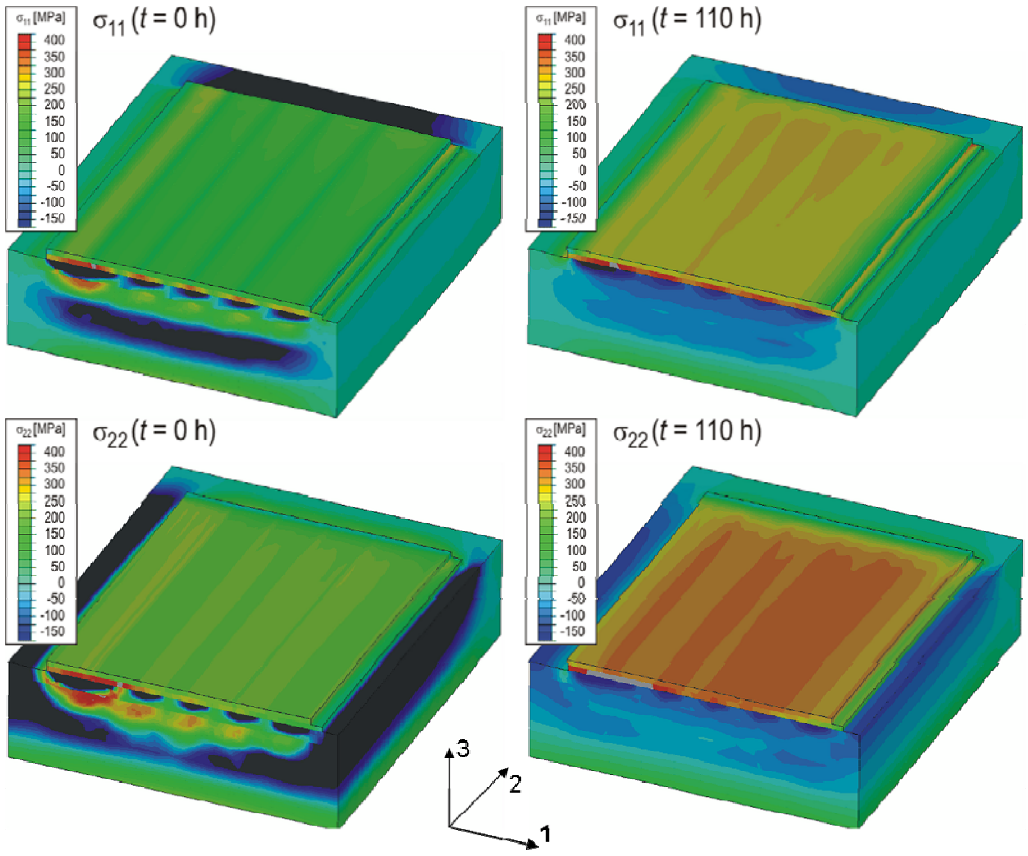

Figure 12: Stress distribution in the plate after welding (on the left) and after PWHT (on the right)

These residual stress results obtained from the welding simulation do not include a post weld heat treatment (PWHT), which significantly reduces the stress levels in the base metal. The numerical simulation of PWHT was performed using visco-elastic-plastic material behavior using the Norton's creep law

$$\frac{\partial \varepsilon_e^{pl}}{\partial t} = A(\sigma_e)^n$$

with the material parameter A and n and ε_e^{pl} and σ_e being the accumulated equivalent plastic strain and the von Mises equivalent stress, respectively. The parameter A and n were determined from the relaxation tests (Figure 5).

The resulting residual stresses distribution after welding and after PWHT is plotted in Figure 12. After PWHT (110 hours: 53 h heating up to 600 °C, 6 h holding at 600 °C, 53 h cooling down) the stress peaks in the base metal a significantly reduced and only compressive stresses remain with a stress level below the cladding of about -50 MPa. On the other hand, in the cladding quite homogeneous tensile stresses of about 300 MPa are present.

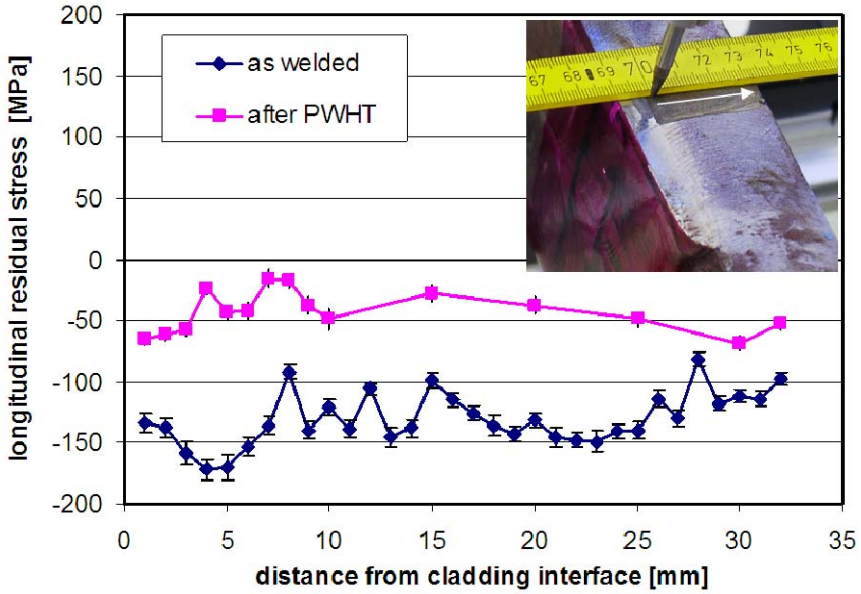

Figure 13: Residual stresses in the base metal before and after PWHT

Figure 13 shows measurements on an additional plate cladded in the same manner using the X-Ray diffraction method. After PWHT the compressive stresses are reduced of about a factor o 3 to about 50 MPa. Also, in the base metal below the cladding only compressive stresses were measured. The results are in good agreement with the results from numerical simulations and results from literature [6].

CONCLUSION

For the determination of the residual stress field due to the cladding process, plates of RPV steel were cladded and heat treated representative to the RPV relevant conditions. During the cladding process temperature profiles were measured as basis for the finite element simulations.

The numerical simulation of the cladding process reveals tensile stresses in the cladding followed by compressive stresses in the base metal that are in agreement with measurements with X-ray diffraction technique. From sensitivity analyses using different mesh densities the accuracy of the complete 3D mesh was qualified. It could be shown that in the cladding process each following strip weld influences the residual stresses in a positive way by a further reduction of the stress level. After PWHT a significant reduction of residual stresses in the base metal is obtained.

ACKNOWLEDGEMENT

This work has been financially supported by the German Federal Ministry of Economics and Technology under grant no. 1501278 in the framework of reactor safety research program.

REFERENCES

1. Blauel, J.G., Hodulak, L., Nagel, G., Schmitt, W., Siegele, D., Effect of cladding on the initiation behavior of finite length cracks in a RPV under thermal shock, Nuclear Engineering and Design, 171 (1997), 179-188.
2. Hodulak, L., Blauel, J.G., Siegele, D., Urich, B., Thermal shock experiments on cracked cladded plates, Nuclear Engineering and Design 188 (1999) p. 139-147.
3. Radaj, D., Residual Stresses and distortion during welding – Calculation and Measurement Procedures (in German), Fachbuchreihe Schweißtechnik Band 143, DVS-Verlag, Düsseldorf 2002, ISBN 3-87155-791-9
4. Keim, E., et al., Life Management of Reactor Pressure Vessels under Pressurized Thermal Shock Loading: Deterministic Procedure and Application to Western and Eastern Type of Reactors, Int. J. Pressure, Vessels and Piping 78 (2001), 85-98.
5. Siegele, D., Varfolomeyev, I., Nagel, G., Investigation on Load Bearing Capacity of the Cladding for Large Crack Postulates under the Cladding of RPV (in German), 27. MPA-Seminar (2001), S. 7.1-7.14.
6. Gripenberg, H., Keinänen, H., Ohms, C., Hänninen, H., Stefanescu, D., and Smith, D., Prediction and Measurement of Residual Stresses in Cladded Steel, Materials science forum, European conference on residual stresses N^{o}6, Coimbra , Portugal (10/07/2002), vol. 404-407, pp. 861-866.
7. Handbook of DVS Recommendations and Guidelines (in German), Deutscher Verband für Schweißtechnik, Düsseldorf 1992, Fachbuchreihe Schweißtechnik Band 109, ISBN 3-87155-126-0
8. Hohe, J. et al, Assessment of cracks in the cladding (in German), Final Report of Reactor Safety Research Project 1501278, IWM Report No. S35/2007, 2007
9. SYSWELD 2008 Reference Manual (C)2007 ESI Group
10. ABAQUS 6.6 User's Manual, ABAQUS Inc., Providence, RI, 2007.
11. Leblond, J. B. & Devaux, J., A new kinetic model for anisothermal metallurgical transformations in steels including effect of austenite grain size, Acta Metallurgica, 1984, Vol. 32, pp 137-146
12. D. P. Koistinen D. P., Marburger R. E., A general equation prescribing extend of austenite-martensite transformation in pure Fe-C alloy and plain carbon steels}, Acta Metallurgica, 1959, Vol. 7, pp 59-60,
13. Brand, M., Further Development of Methods of Numerical Welding Simulation, PhD-Thesis, in progress, (in German)